

Unsteady Mixed Convection Slip Flow around a Stretching Sheet in Porous Medium

Md. Aminul Islam^{1,2*}, Md. Yeakub Ali¹, Romena Akter^{1,2}, S. M. Osman Gani^{1,2}

¹Department of Mathematics, Chittagong University of Engineering & Technology, Chattogram, Bangladesh

²Department of Natural Science, Port City International University, Chattogram, Bangladesh

Email: *aminulislampciu88@gmail.com

How to cite this paper: Islam, M.A., Ali, M.Y., Akter, R. and Gani, S.M.O. (2022) Unsteady Mixed Convection Slip Flow around a Stretching Sheet in Porous Medium. *Journal of Applied Mathematics and Physics*, 10, 3016-3036.
<https://doi.org/10.4236/jamp.2022.1010202>

Received: August 27, 2022

Accepted: October 16, 2022

Published: October 19, 2022

Copyright © 2022 by author(s) and Scientific Research Publishing Inc.

This work is licensed under the Creative Commons Attribution International License (CC BY 4.0).

<http://creativecommons.org/licenses/by/4.0/>



Open Access

Abstract

The heat and mass transfer of unsteady MHD two-dimensional mixed convection boundary layer flow over an exponentially porous stretching sheet is presented in this paper. Multiple slip conditions, radiation, suction or blowing, heat generation or absorption along with magnetism and porous medium are incorporated. We reduce the leading equations which are partial differential equations into a family of ordinary differential equations that are non-linear using a set of similarity transformations. The resulting equations with coupled boundary conditions are solved numerically with the aid of bvp4c solver with MATLAB package. The impacts of several non-dimensional governing parameters on the flow fields such as velocity, temperature and concentration profiles along with friction coefficient, temperature gradient and concentration gradient are portrayed graphically and discussed in detail. The result indicates that the magnetic parameter decreases the skin friction coefficient. Thermal boundary layer thickness reduces with increasing radiation parameters and enhances with increasing Prandtl number. It is also observed that the thermal slip parameter depreciates the heat transfer rate and the mass slip parameter diminishes the mass transfer rate. A comparison has been made between the current results and the numerical results of previous studies and observed a very close good agreement.

Keywords

Mixed Convection, Porous Medium, Slips Boundary Conditions, Suction/Blowing

1. Introduction

If natural convection is combined with forced convection, then the resulting convection is known as mixed convection, which is frequently used to get the

desired result when the forced convection can't dissipate all the heat in the devices involving high voltage. There are several industrial and technical applications of mixed convection including the cooling of nuclear reactors during an emergency shutdown, a heat exchanger placed in a low-velocity environment, solar collectors, electronic devices cooled by fans, etc. [1]. Srinivasacharya and RamReddy [2] investigated the problem of mixed convection boundary flow, heat and mass transfer over an exponentially stretching sheet in the presence of Soret and Dufour. Aman and Ishak [3] studied the mixed convection boundary layer flow and heat transfer over an impermeable vertical plate, taking convective thermal conditions at the boundary. Isa *et al.* [4] described joule heating effects on MHD mixed convection flow past an exponentially stretching vertical sheet with viscous dissipation, heat generation and convective boundary condition. Patil *et al.* [5] obtained a non-similar solution of mixed convection boundary layer flow, heat and mass transfer over a vertical semi-infinite impermeable exponentially stretching surface with first order chemical reaction. Ali *et al.* [6] described the effects of thermal radiation on two-dimensional mixed convection stagnation point flow and heat transfer over a vertical stretching sheet in the presence of the external magnetic field.

The study of porous media with heat transfer has attracted the attention of researchers due to its wide applications in applied science, soil mechanics, rock mechanics, petroleum engineering, construction engineering, geoscience and many more. For example, food processing, cooling of nuclear reactors, underground disposal of nuclear waste, underground water resources and seepage of water in river beds in agricultural engineering, petroleum reservoir operations, filtration and purification in chemical engineering, building insulation, and casting and welding in manufacturing processes, etc. [7] [8]. Several investigators studied the combined effects of heat and mass transfer in mixed convection through porous medium under different conditions. Afify and Elgazery [9] studied the combined effects of thermal radiation, melting and double dispersion on the non-Darcy mixed convective boundary layer flow, heat and mass transfer over a vertical porous surface using Chebyshev pseudo spectral method. Tripathy *et al.* [10] described the effects of a non-uniform heat source and chemical reaction on the convected flow, heat and mass transfer of a micropolar fluid along a stretching sheet embedded in a porous medium. Nithyadevi *et al.* [11] presented the problem of MHD mixed convection flow of a nano fluid numerically in a vertically lid-driven porous enclosure with a center heater. Krishna *et al.* [12] studied the combined effects of chemical reaction, hall and ion slip on unsteady MHD free convective rotating flow, heat and mass transfer over an exponentially accelerated inclined plate in a porous medium.

Nowadays, researchers have considered unsteady two-dimensional boundary layer flow under different conditions due to its importance in many engineering processes. The flow fields become unsteady as a result of a sudden change in the surface temperature, and impulsive stretching of the surface or external stream [13].

The study of heat generation or absorption is important in heat and mass transfer in certain porous media applications. The temperature distribution may be changed with the effects of heat generation. Therefore, the particle deposition rate is affected in nuclear reactors, electronic chips, and semiconductor wafers [14]. Moreover, radiative heat transfer is significant in processes involving high temperatures.

The problem of the slip flow regime is extremely important in this area of recent science, technology and immense extending automation. The fluid slippage phenomenon at the solid boundaries appears in many applications like micro channels or Nano channels. It is also used where a thin film of light oils is involved in the moving plates or when the surfaces are coated with special coating to lessen the friction between them [15]. The flow field can be changed significantly through the bounding surface with the suction or blowing of a fluid. Generally, suction has a tendency to increase skin friction, whereas the reverse occurs with blowing. Blowing or removal of fluid through a porous bounding wall is of general attention in practical problems including boundary layer control applications such as film cooling, polymer fibre coating, and coating of wires [16]. Mukhopadhyay [17] analyzed the slip effects on unsteady mixed convection flow over a stretching surface with suction. Sreelakshmi and Nagendramma [18] studied the influence of thermophoresis, viscous dissipation and temperature dependent heat source on the unsteady boundary layer flow of a viscous fluid over an exponentially stretching sheet with chemical reaction. Mabood and Shateyi [19] described the combined effect of Soret and thermal radiation on unsteady MHD mixed convection flow over a stretching sheet with suction and slip boundary conditions. Through porous medium, unsteady MHD boundary layer slip flow over an exponentially stretching sheet including radiation, heat generation, and suction was analyzed numerically by Islam *et al.* [20].

As far as is known no studies have been described on the unsteady MHD mixed convection heat and mass transfer flow over a porous radiative sheet which stretches exponentially with heat generation or absorption, suction and slip boundary conditions by considering $L = 1$ and $\alpha = 1$ in the similarity and dimensionless variables. We convert the governing partial differential equations to a group of nonlinear ordinary differential equations using similarity transformations. Numerical solutions of those equations are found using the `bvp4c` function in MATLAB software.

2. Formulation of the Problem

We study an unsteady, laminar, two-dimensional, incompressible and electrically conducting MHD mixed convection boundary layer flow in a porous medium with slip boundary conditions. We select a cartesian co-ordinate system such that the x-axis is along the sheet and y-axis is normal to it. The surface is stretched with the velocity $U(x,t) = \frac{U_0}{1-t}e^x$, temperature distribution

$$T_w(x, t) = T_\infty + \frac{T_0}{(1-t)^2} e^{x/2} \quad \text{and concentration distribution}$$

$$C_w(x, t) = C_\infty + \frac{C_0}{(1-t)^2} e^{x/2}, \quad \text{where } U_0, T_0 \text{ and } C_0 \text{ denote the reference velocity,}$$

temperature and concentration respectively, T_∞ and C_∞ represent the ambient temperature and concentration respectively with $T_w > T_\infty$ and $C_w > C_\infty$. It is worth mentioning that we take $L=1$ and $\alpha=1$ in similarity and dimensionless variables. The flow is produced by the sheet stretching in the exponential form.

The equations of conservation of mass, momentum, energy and species concentration governing the mixed convection boundary layer flow over a porous exponential stretching sheet can be written as:

$$\frac{\partial u}{\partial x} + \frac{\partial v}{\partial y} = 0 \quad (1)$$

$$\begin{aligned} & \frac{\partial u}{\partial t} + u \frac{\partial u}{\partial x} + v \frac{\partial u}{\partial y} \\ & = \nu \frac{\partial^2 u}{\partial y^2} + g \beta_T (T - T_\infty) + g \beta_C (C - C_\infty) - \frac{\sigma B^2}{\rho} u - \frac{\nu}{K_1} u \end{aligned} \quad (2)$$

$$\frac{\partial T}{\partial t} + u \frac{\partial T}{\partial x} + v \frac{\partial T}{\partial y} = \frac{\kappa}{\rho C_p} \frac{\partial^2 T}{\partial y^2} - \frac{1}{\rho C_p} \frac{\partial q_r}{\partial y} + \frac{1}{\rho C_p} Q_0 (T - T_\infty) \quad (3)$$

$$\frac{\partial C}{\partial t} + u \frac{\partial C}{\partial x} + v \frac{\partial C}{\partial y} = D_m \frac{\partial^2 C}{\partial y^2} \quad (4)$$

with the corresponding boundary conditions:

$$\begin{aligned} u &= U(x, t) + Nv \frac{\partial u}{\partial y}, \quad V = -V(x, t), \quad T = T_w(x, t) + E \frac{\partial T}{\partial y}, \\ C &= C_w(x, t) + F \frac{\partial C}{\partial y}, \quad \text{at } y = 0 \\ \text{and } u &\rightarrow 0, T \rightarrow T_\infty, C \rightarrow C_\infty \quad \text{as } y \rightarrow \infty \end{aligned} \quad (5)$$

where the components of velocity in x and y directions are represented by u , v respectively, t denotes the time, ρ stands for the density and kinematic viscosity, gravitational acceleration, thermal expansion coefficient, the temperature of the fluid, mass expansion coefficient, concentration and electric conductivity of the fluid are indicated by ν , g , β_T , T , β_C , C and σ respectively. Moreover, κ is for the thermal conductivity, C_p represents the specific heat at constant pressure, the radiative heat flux is expressed by q_r and the co-efficient of heat generation and mass diffusivity are denoted by Q_0 and D_m respectively. Further, the uniform magnetic field, the permeability of the porous medium, the suction or injection velocity and velocity, thermal and mass slip factors are defined as follows:

$$\begin{aligned} B(t) &= B_0 (1-t)^{-1/2} e^{x/2}, \quad K_1 = K_0 (1-t) e^{-x}, \quad V(x, t) = V_0 (1-t)^{-1/2} e^{x/2} \\ N &= N_1 (1-t)^{1/2} e^{-x/2}, \quad E = E_1 (1-t)^{1/2} e^{-x/2}, \quad F = F_1 (1-t)^{1/2} e^{-x/2}. \end{aligned}$$

Here B_0 is the intensity of magnetic field, K_0 is a constant, V_0 is the strength of suction or blowing, N_1 stands for the initial values of velocity slip factor, E_1 denotes the initial values of thermal slip factor and F_1 characterizes the initial values of mass slip factor. We can attain the condition of the no-slip condition considering $N = E = F = 0$.

The q_r , known as radiative heat flux through Rosseland approximation [21], is as follows:

$$q_r = -\frac{4\sigma^*}{3K^*} \frac{\partial T^4}{\partial y} \tag{6}$$

Here σ^* signifies the Stefan-Boltzman constant and K^* stand for the absorption coefficient. If the difference in the temperature within the flow is sufficiently small then we can expand T^4 in Taylor's series about T_∞ . If we neglect the higher order terms except the first degree in $(T - T_\infty)$ then we get $T^4 \cong 4T_\infty^3 T - 3T_\infty^4$.

Then the Equation (3) can be written as follows:

$$\frac{\partial T}{\partial t} + u \frac{\partial T}{\partial x} + v \frac{\partial T}{\partial y} = \frac{\kappa}{\rho C_p} \frac{\partial^2 T}{\partial y^2} + \frac{1}{\rho C_p} \frac{16\sigma^* T_\infty^3}{3K^*} \frac{\partial^2 T}{\partial y^2} + \frac{1}{\rho C_p} Q_0 (T - T_\infty) \tag{7}$$

Introducing the dimensionless variables as:

$$\begin{aligned} \eta &= \sqrt{\frac{U}{2\nu}} y, \psi = \sqrt{2\nu U} f(\eta) \\ \theta(\eta) &= \frac{T - T_\infty}{T_w - T_\infty}, \phi(\eta) = \frac{C - C_\infty}{C_w - C_\infty} \end{aligned} \tag{8}$$

and upon replacement of (8) in the Equations (2), (3) and (4), a family of nonlinear ordinary differential equations are obtained as follows:

$$f''' + ff'' - 2f'^2 - Ae^{-X}(2f' + \eta f'') + Gr\theta + Gc\phi - (M + K)f' = 0 \tag{9}$$

$$\left(1 + \frac{4}{3}R\right)\theta'' + Pr(f\theta' - f'\theta) - Pre^{-X}A(4\theta + \eta\theta') + Pre^{-X}Q_H\theta = 0 \tag{10}$$

$$\phi'' + Sc[(f\phi' - f'\phi) - e^{-X}A(4\phi + \eta\phi')] = 0 \tag{11}$$

and the Equation (5) representing boundary conditions, is simplified as follows:

$$\begin{aligned} f(0) &= S, f'(0) = 1 + \lambda f''(0), \theta(0) = 1 + \delta\theta'(0), \\ \phi(0) &= 1 + \gamma\phi'(0) \text{ at } \eta = 0 \\ \text{and } f'(\infty) &\rightarrow 0, \theta(\infty) \rightarrow 0, \phi(\infty) \rightarrow 0 \text{ as } \eta \rightarrow \infty \end{aligned} \tag{12}$$

where $X = x$ is the dimensionless co-ordinate, $A = \frac{1}{U_o}$ is the unsteadiness

parameter, $Gr = \frac{2g\beta_T(T_w - T_\infty)}{U^2}$ is the thermal Grashof number,

$Gr = \frac{2g\beta_c(C_w - C_\infty)}{U^2}$ mass Grashof number, $Re_x = \frac{xU}{\nu}$ is the local Reynolds

number, $M = \frac{2\sigma B_0^2}{\rho U_o}$ is the magnetic parameter, $K = \frac{2\nu}{K_0 U_o}$ is the permeability

of the porous medium, $R = \frac{4\sigma^* T_\infty^3}{\kappa K^*}$ is the radiation parameter, $Q_H = \frac{Q_0(1-t)}{U_0 \rho C_p}$ is the heat generation parameter for $Q_H > 0$ and absorption parameter for $Q_H < 0$, $Pr = \frac{\rho C_p \nu}{\kappa}$ is the Prandtl number, $Sc = \frac{\nu}{D_m}$ is the Schmidt number, $S = \frac{V_0}{\sqrt{\frac{U_0 \nu}{2}}}$ is the suction parameter, $\lambda = N_1 \sqrt{\frac{U_0 \nu}{2}}$ is the velocity slip parameter, $\delta = E_1 \sqrt{\frac{U_0}{2\nu}}$ is the thermal slip parameter and the mass slip parameter is denoted by $\gamma = F_1 \sqrt{\frac{U_0}{2\nu}}$ and the prime symbolizes the derivative w.r.t η . The physical quantities of interest in this problem are C_f known as Skin-friction co-efficient, N_{u_x} known as Nusselt number and S_{h_x} known as Sherwood number, defined as follows:

$$C_f = \frac{2\tau_w}{\rho U^2} = \sqrt{2x} (Re_x)^{-\frac{1}{2}} f''(0) \quad (13)$$

$$N_{u_x} = \frac{xq_w}{k(T_w - T_\infty)} = -\sqrt{\frac{x}{2}} \sqrt{Re_x} \theta'(0) \quad \text{and} \quad (14)$$

$$S_{h_x} = \frac{xJ_w}{D(C_w - C_\infty)} = -\sqrt{\frac{x}{2}} \sqrt{Re_x} \phi'(0) \quad (15)$$

3. Result and Discussions

In this study, an investigation is carried out to illustrate graphically the effects of different non-dimensional physical parameters on the velocity, temperature and concentration profiles taking $X = 2$, $\eta = 2$, $Gr = Gc = K = Q_H = 0.1$, $M = S = 0.5$, $Pr = 5$, $Sc = 1.5$, $R = A = \delta = \gamma = 0.3$ and $\lambda = 0.05$. In **Table 1**, we compare the value of Skin-friction co-efficient $f(0)$ for unsteadiness parameter A with the results of Mabood and Shateyi [19] and find a close good agreement. In **Table 2**, a comparison of the value of Skin-friction co-efficient $f(0)$ for some values of magnetic parameter M with the results of Mabood and Shateyi [19] is presented and it is observed that an excellent agreement exists. We also see from **Table 2** that skin-friction co-efficient reduces for large values of magnetic parameter M . **Table 3** is tabulated to compare the values of Nusselt number for some values of Prandtl number Pr with the results of Mabood and Shateyi [19] and Srinivasacharya and RamReddy [2]. We see that our results are very close to the previously published results. From these comparisons which are shown in **Tables 1-3**, we can assure that our present research work is valid and accurate.

The effects of thermal Grashof number (Gr) which is the ratio of the buoyancy force to the viscous force acting on the fluid, on velocity, temperature and concentration profiles are illustrated in **Figures 1-3** respectively. It is noticed that velocity decreases as the thermal Grashof number increases, whereas temperature

Table 1. Comparison of the value of Skin-friction co-efficient $f''(0)$ for unsteadiness parameter A .

A	Mabood and Shateyi [19]	Present result
0.8	-1.261042	-1.2904

Table 2. Comparison of the value of Skin-friction co-efficient $f''(0)$ for some values of magnetic parameter M when $X = S = A = \lambda = K = Q_H = 0$.

M	Mabood and Shateyi [19]	Present result
5	-2.44948974	-2.6592
10	-3.31662479	-3.4617
50	-7.14142843	-7.2126
100	-10.0498756	-10.1025
500	-22.3830293	-22.4082
1000	-31.6385840	-31.6567

Table 3. Comparison of the value of Nusselt number $[-\theta'(0)]$ for some values of Prandtl number Pr when $X = Gr = Gc = K = Q_H = M = S = Sc = R = A = \delta = \gamma = \lambda = 0$.

Pr	Mabood and Shateyi [19]	Srinivasacharya and RamReddy [2]	Present result
3	1.9237	1.86908	1.9355
5	-	2.50015	2.4684
8	-	3.24218	3.1641
10	3.7207	3.66043	3.5739

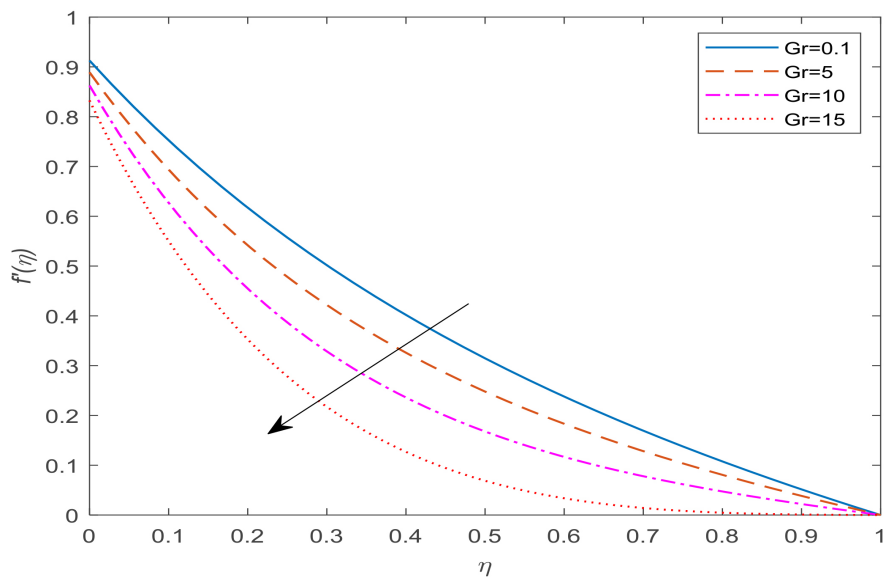


Figure 1. Influence of Gr on velocity profile $f'(\eta)$.

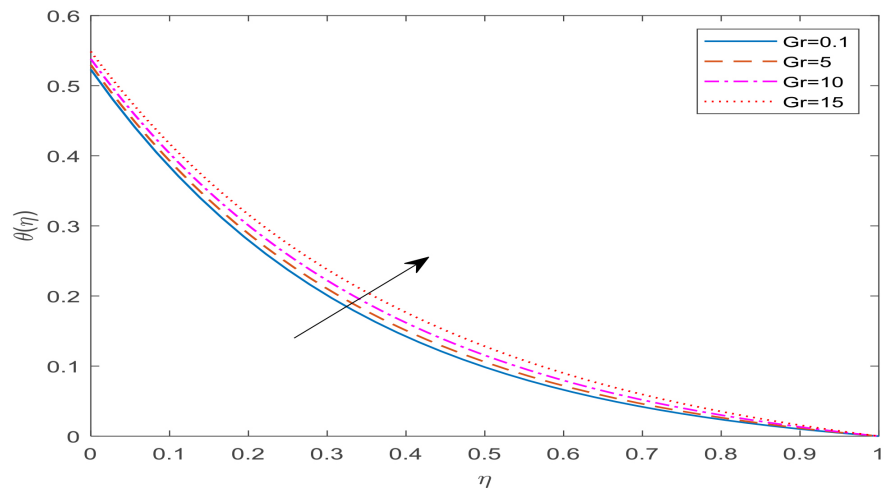


Figure 2. Impact of Gr on temperature profile $\theta(\eta)$.

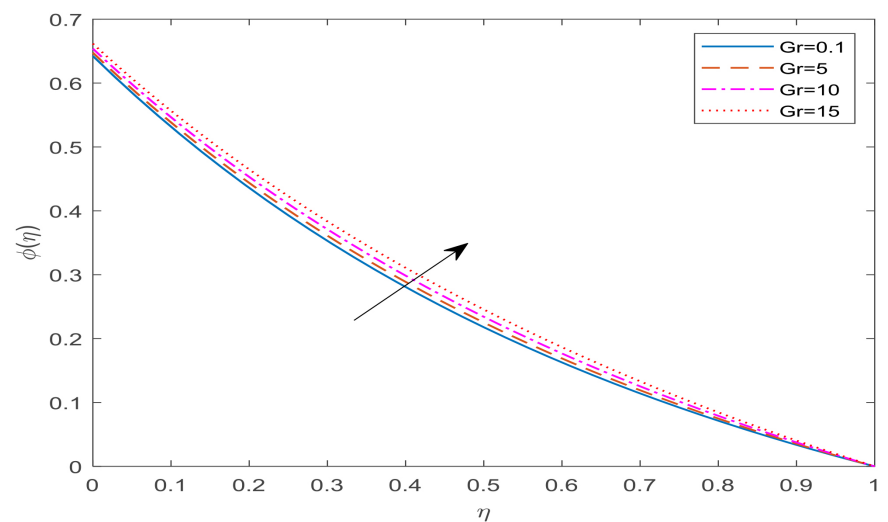


Figure 3. Influence of Gr on concentration profile $\phi(\eta)$.

and concentration enhance with the rise in thermal Grashof number (Gr) respectively. The boundary layer flow becomes laminar and contrarywise at higher thermal Grashof numbers. The ratio of the solutal buoyancy force to the viscous hydrodynamic is known as the solutal Grashof number (Gc). **Figures 4-6** reveal the influence of solutal Grashof number (Gc) on velocity, temperature and concentration profiles respectively. It is also observed that fluid velocity decreases and temperature and concentration increase with the increasing values of solutal Grashof number (Gc). **Figures 7-9** describes the effects of magnetic parameter on velocity, temperature and concentration profiles respectively. It is seen from **Figure 7** that fluid velocity reduces with the rise in magnetic parameters. This happens because of a resistive force named Lorenz force which is produced due to the imposed magnetic field. On the other hand, temperature and concentration profiles are seen to enhance the rising values of the magnetic parameter.

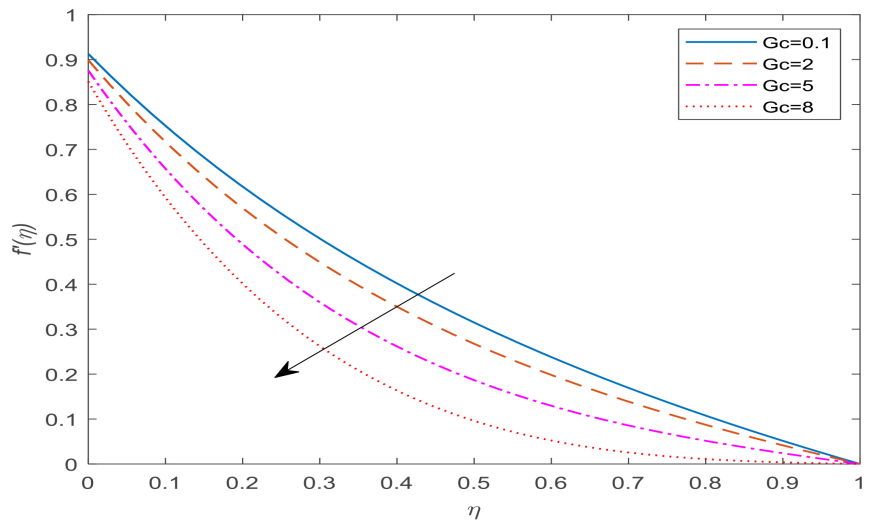


Figure 4. Influence of Gc on velocity profile $f'(\eta)$.

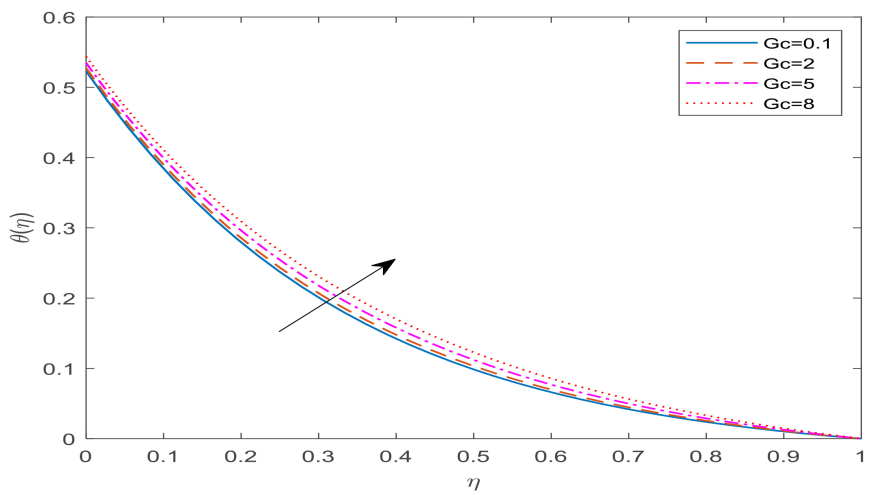


Figure 5. Influence of Gc on temperature profile $\theta(\eta)$.

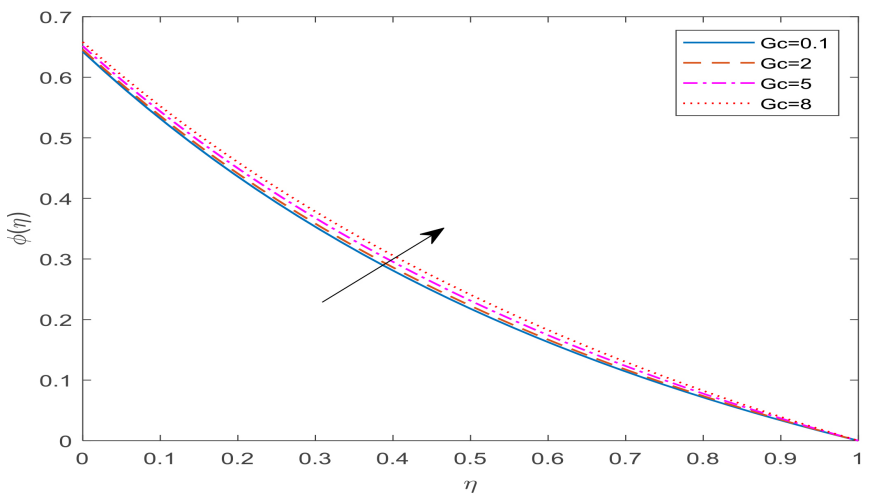


Figure 6. Influence of Gc on concentration profile $\phi(\eta)$.

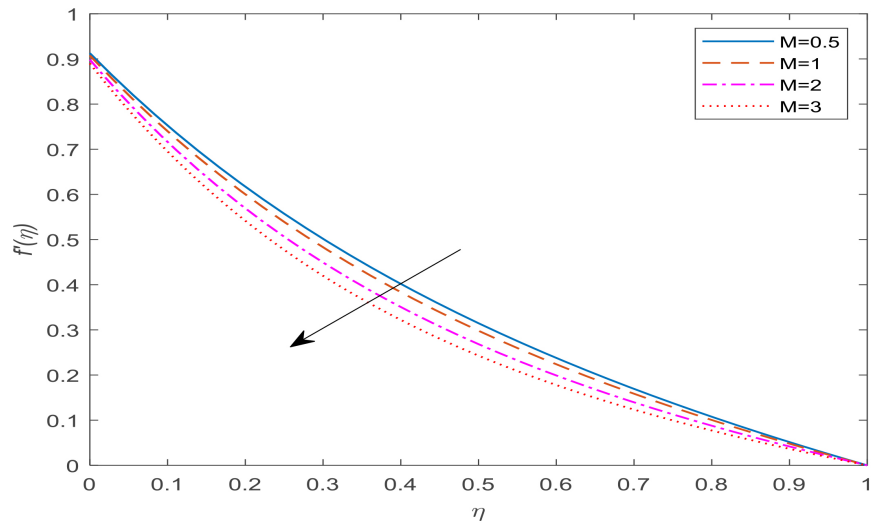


Figure 7. Influence of M on velocity profile $f'(\eta)$.

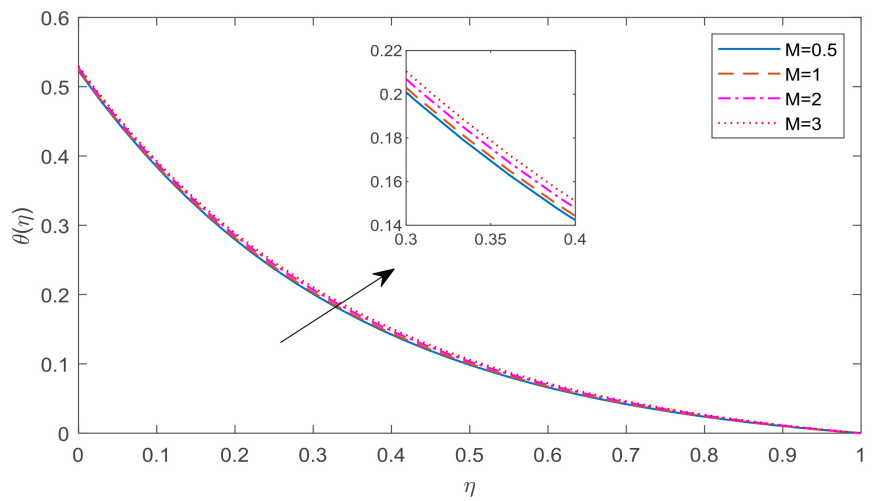


Figure 8. Influence of M on temperature profile $\theta(\eta)$.

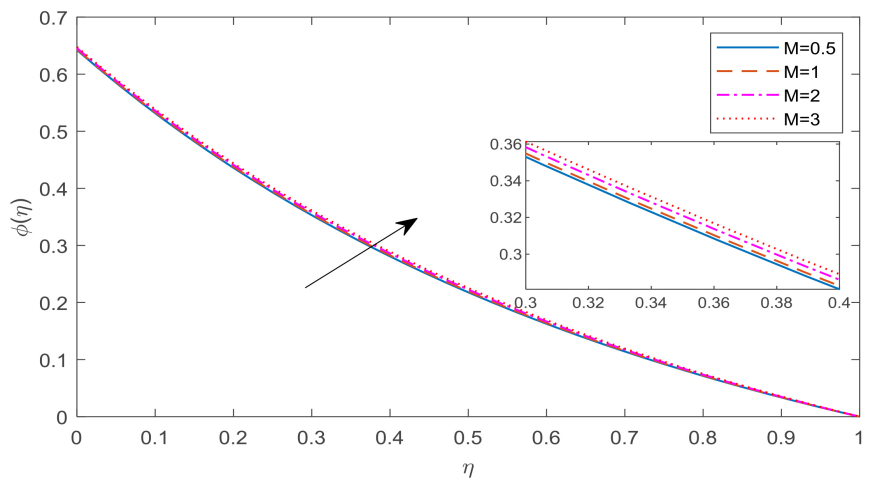


Figure 9. Influence of M on concentration profile $\phi(\eta)$.

For various values of porosity parameter (K), the velocity, temperature and concentration distribution are plotted in **Figures 10-12**. It is understood from **Figure 10** that increasing values of porosity parameter decline the fluid velocity and therefore decrease the momentum boundary layer thickness. As like magnetic parameter, temperature and concentration distribution (**Figure 11** & **Figure 12**) decrease as porosity parameter (K) increases.

Figures 13-15 clarify the effects of the unsteadiness parameter on velocity, temperature and concentration profiles respectively. As the unsteadiness parameter increases fluid velocity, temperature and concentration profiles increase respectively. **Figures 16-18** elucidate the effects of velocity slip parameter on velocity, temperature and concentration profiles respectively. It is noticed from **Figure 16** that velocity profile reduces as the velocity slip parameter rises. With the increasing values of velocity slip parameter, the slip velocity increases and so

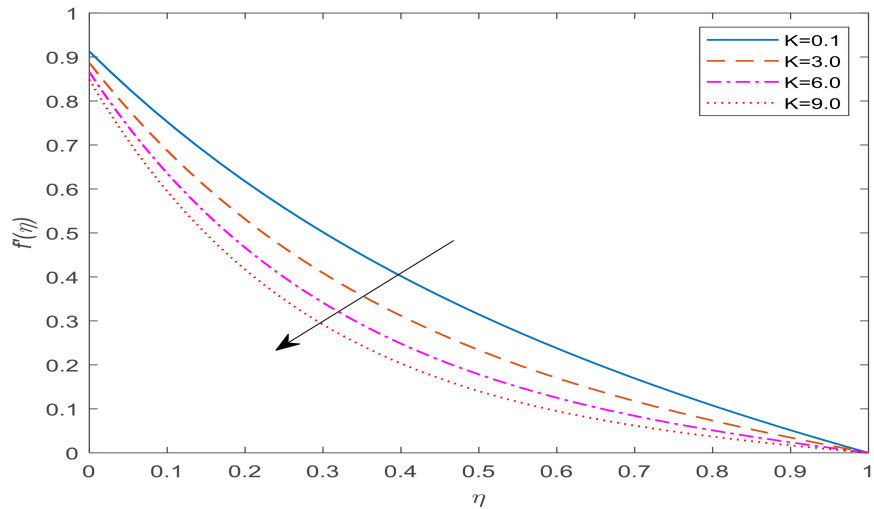


Figure 10. Influence of K on velocity profile $f'(\eta)$.

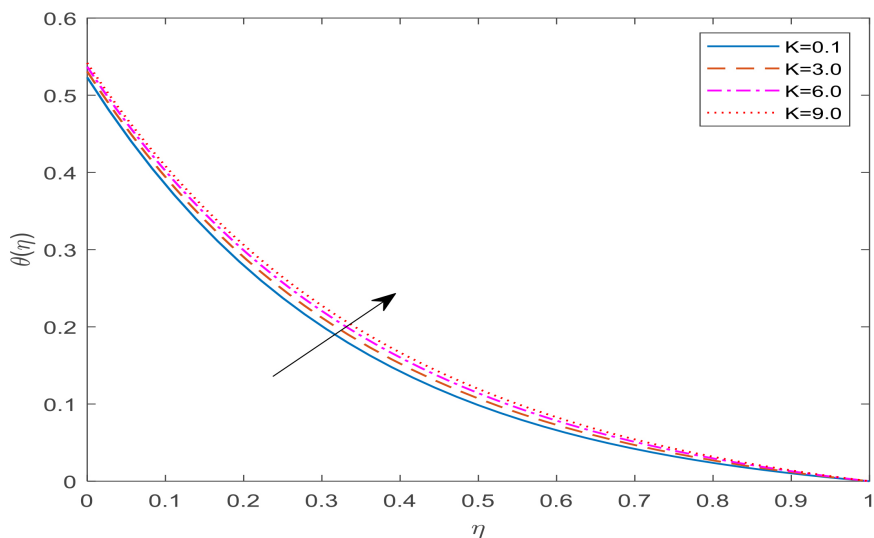


Figure 11. Influence of K on temperature profile $\theta(\eta)$.

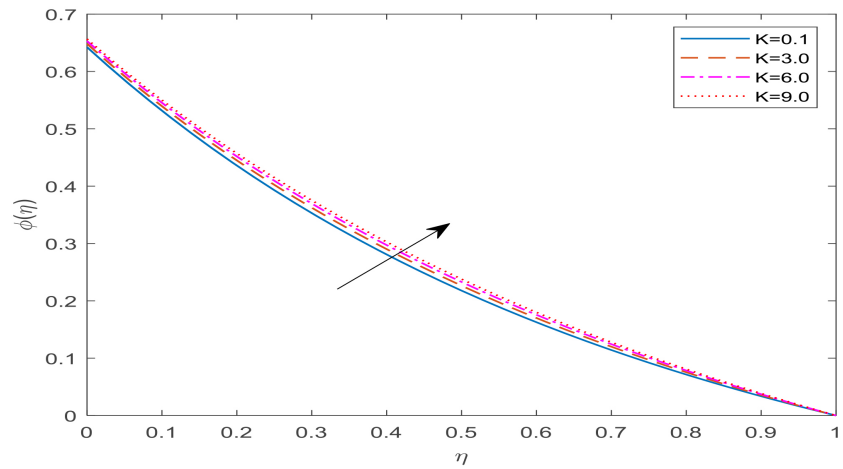


Figure 12. Influence of K on concentration profile $\phi(\eta)$.

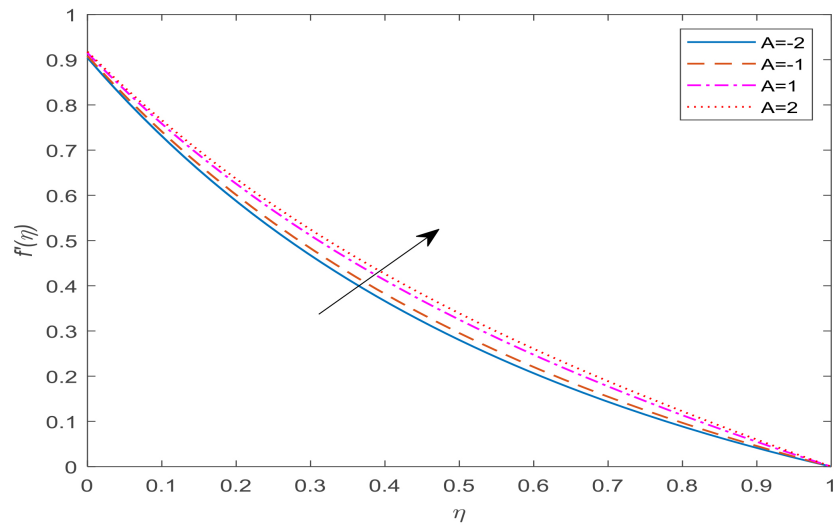


Figure 13. Influence of A on velocity profile $f'(\eta)$.

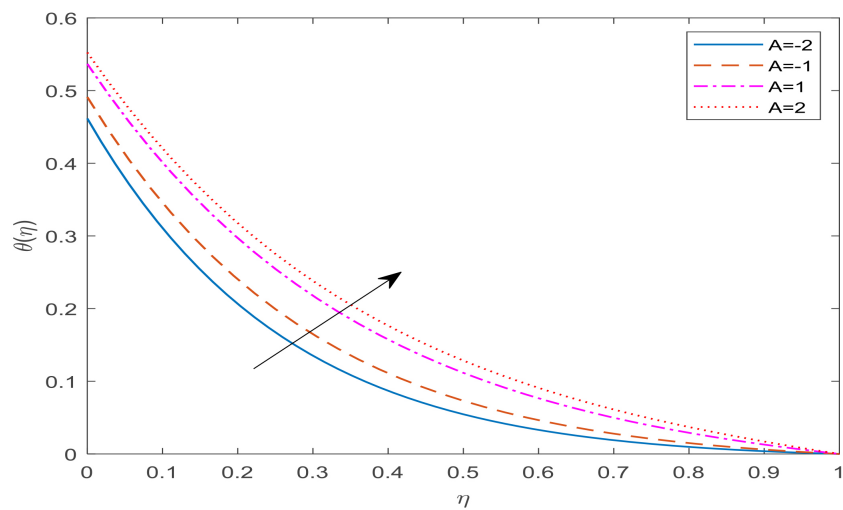


Figure 14. Influence of A on temperature profile $\theta(\eta)$.

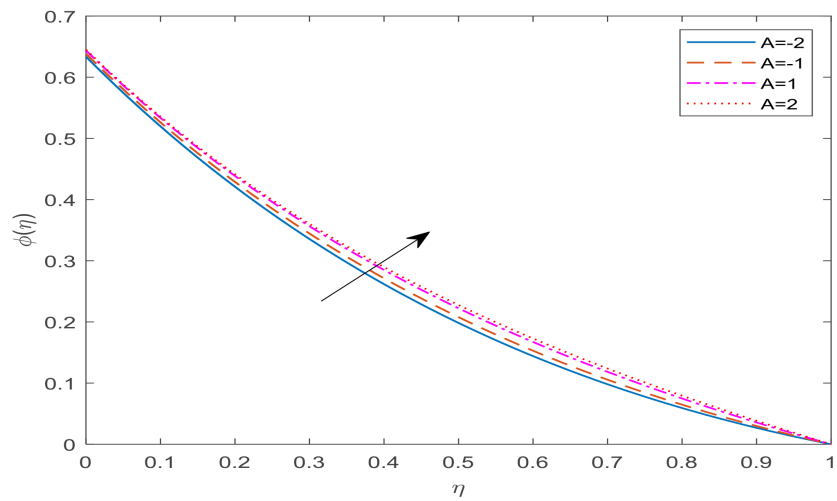


Figure 15. Influence of A on concentration profile $\phi(\eta)$.

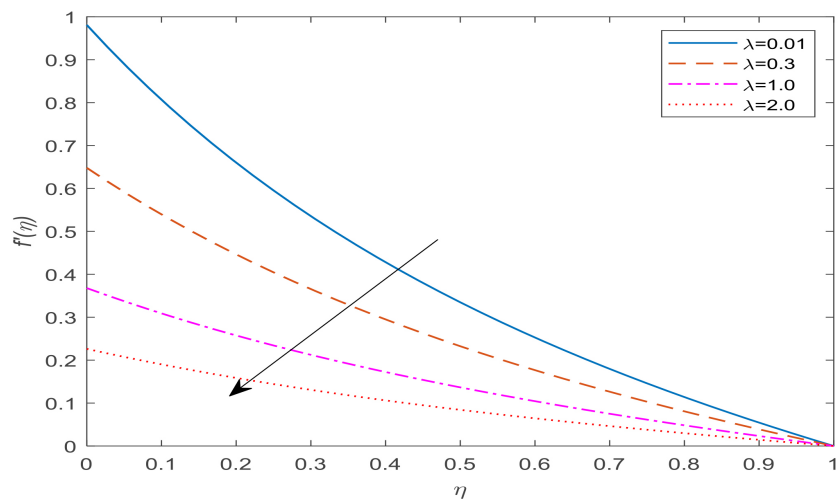


Figure 16. Influence of λ on velocity profile $f'(\eta)$.

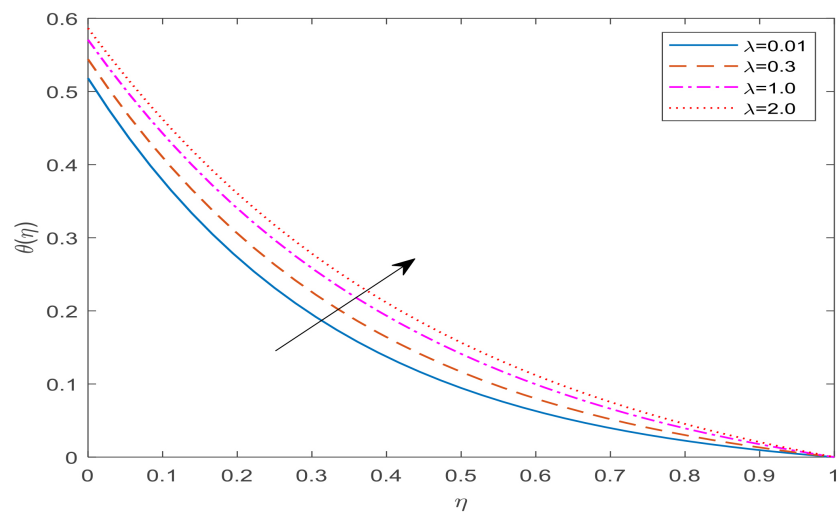


Figure 17. Influence of λ on temperature profile $\theta(\eta)$.

the fluid velocity reduces. It is also seen from **Figure 17** & **Figure 18** that temperature and concentration graphs rise as the value of velocity slip parameter (λ) enhances.

Figure 19 demonstrates the effects of Prandtl number (Pr) on temperature profile. The fluid temperature decreases when the Prandtl number increases. An increment in the Prandtl number has a tendency to increase fluid viscosity which reduces temperature along with thermal boundary layer thickness. **Figure 20** presents that fluid temperature increases due to increase in radiation parameter. Because heat transfer increases with the rise of radiation parameter (R). **Figure 21** exhibits the influence of heat generation and absorption parameter on temperature profile. It is seen that heat generation ($Q_H > 0$) parameter increases the fluid temperature by increasing the thermal boundary layer thickness whereas

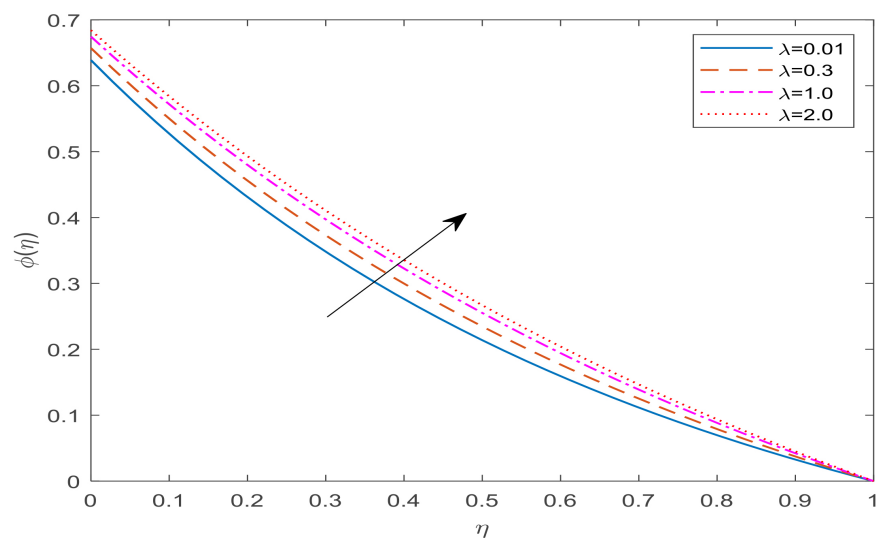


Figure 18. Influence of λ on concentration profile $\phi(\eta)$.

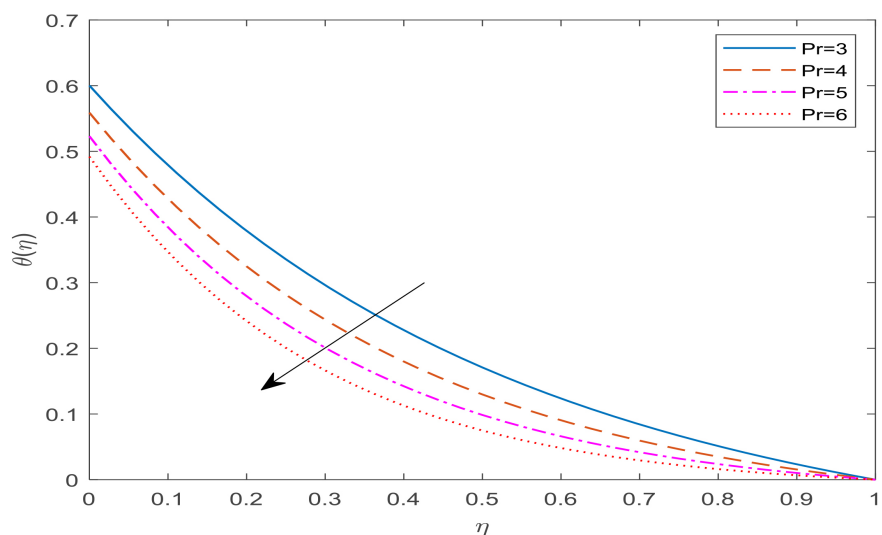


Figure 19. Influence of Pr on temperature profile $\theta(\eta)$.

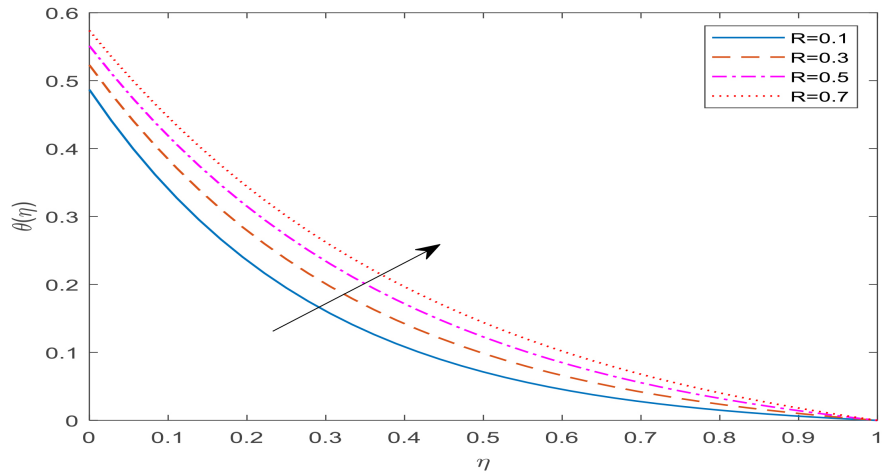


Figure 20. Influence of R on temperature profile $\theta(\eta)$.

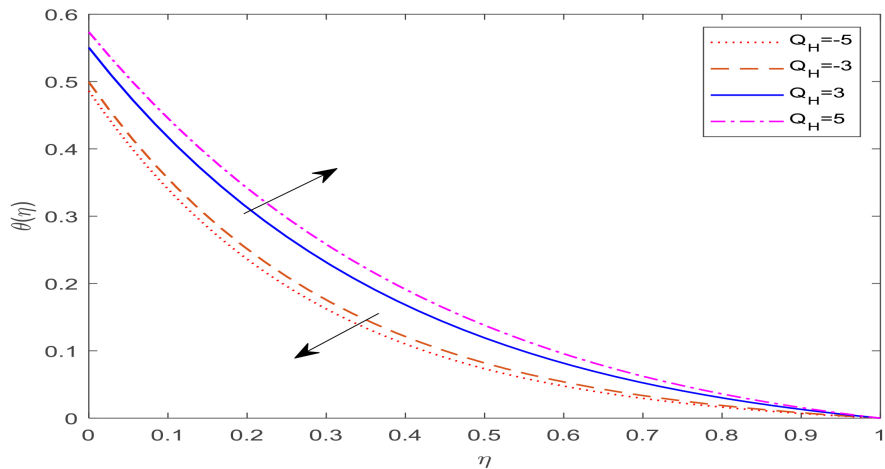


Figure 21. Influence of Q_H on temperature profile $\theta(\eta)$.

the temperature is an increasing function of heat absorption parameter ($Q_H < 0$). The influence of thermal slip parameter on temperature profile is displayed in **Figure 22**, which shows that temperature decreases with the increasing values of thermal slip parameter (δ). Schmidt number which is a dimensionless number, varies inversely to mass diffusivity. So, concentration distribution declines with larger values of Schmidt (Sc) as shown in **Figure 23**. It is interesting to note from **Figure 24** that mass slip parameter has the same effects on concentration pattern as that of thermal slip parameter, that is, concentration distribution decelerates with an increment in the mass slip parameter (γ).

Figures 25-27 show the effects of suction and blowing parameter on velocity, temperature and concentration profiles respectively. It is noticed that with the increasing values of suction parameter ($S > 0$) velocity, temperature and concentration graph decrease respectively while opposite effect is seen for blowing parameter ($S < 0$). **Figure 28** is constructed to describe the impact of thermal Grashof number on shear stress. We notice that skin friction coefficient reduces initially

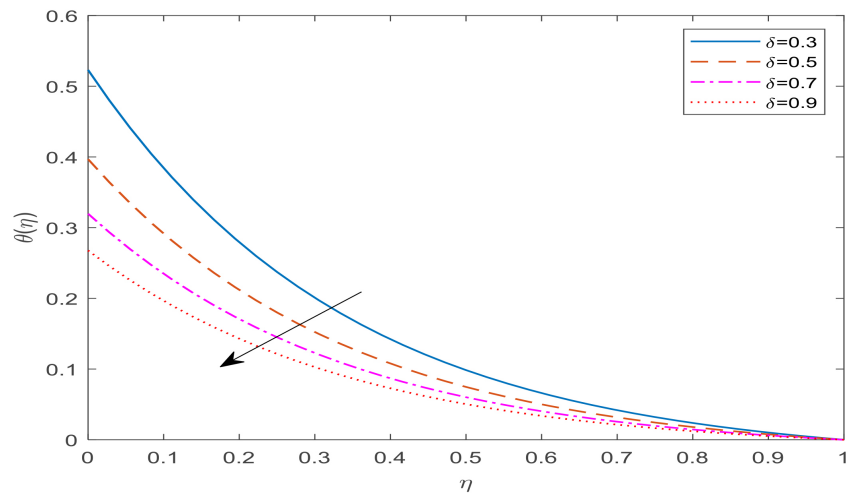


Figure 22. Influence of δ on temperature profile $\theta(\eta)$.

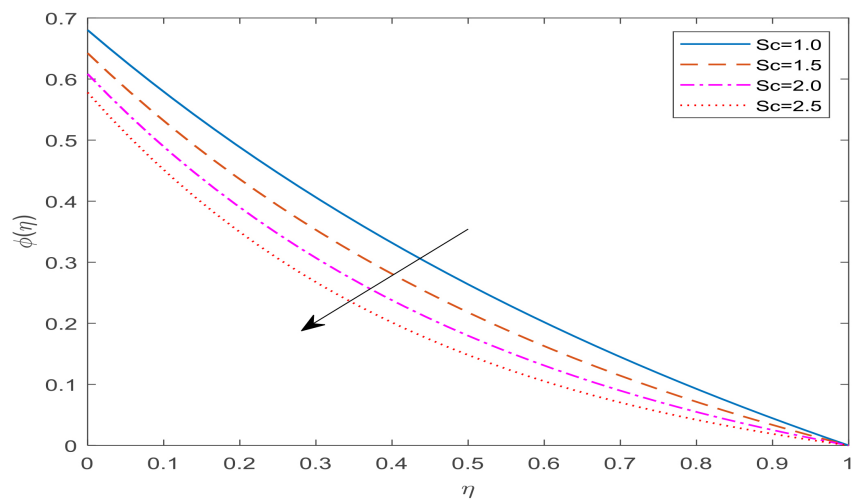


Figure 23. Influence of Sc on concentration profile $\phi(\eta)$.

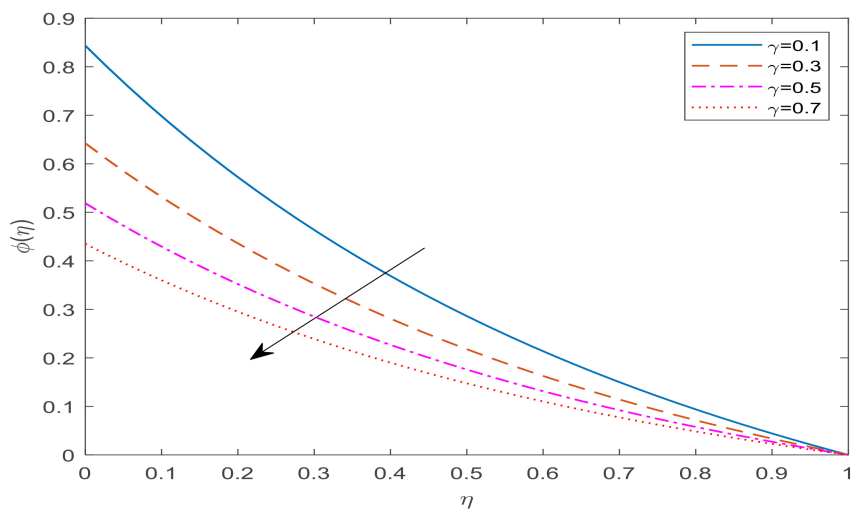


Figure 24. Influence of γ on concentration profile $\phi(\eta)$.

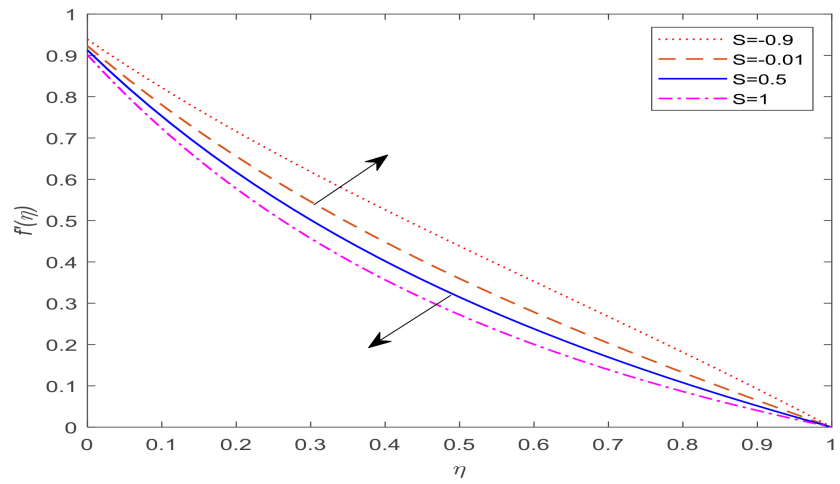


Figure 25. Influence of S on velocity profile $f'(\eta)$.

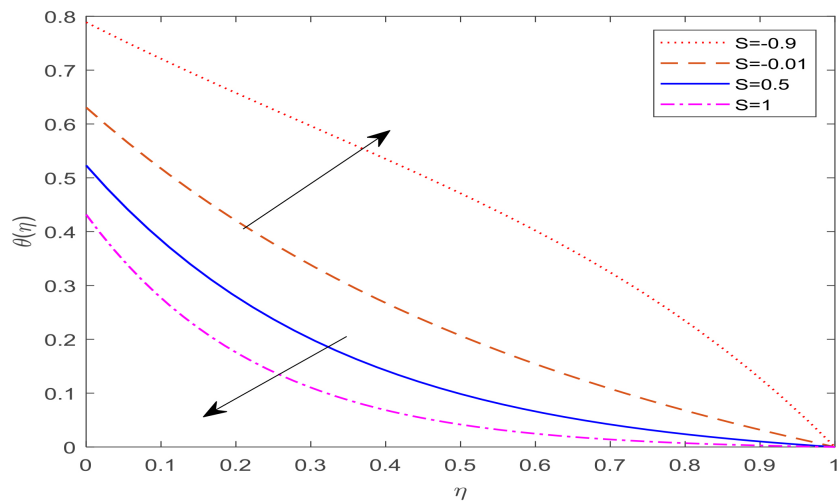


Figure 26. Influence of S on temperature profile $\theta(\eta)$.

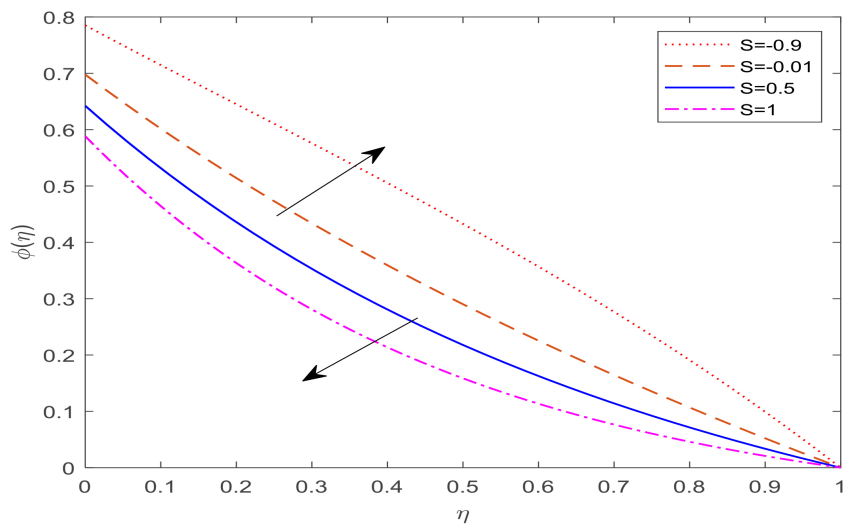


Figure 27. Influence of S on concentration profile $\phi(\eta)$.

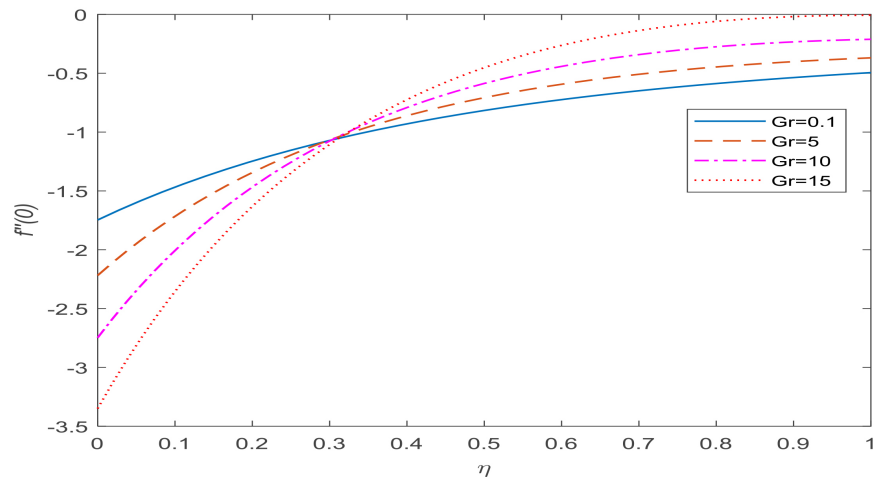


Figure 28. Influence of Gr on skin friction coefficient.

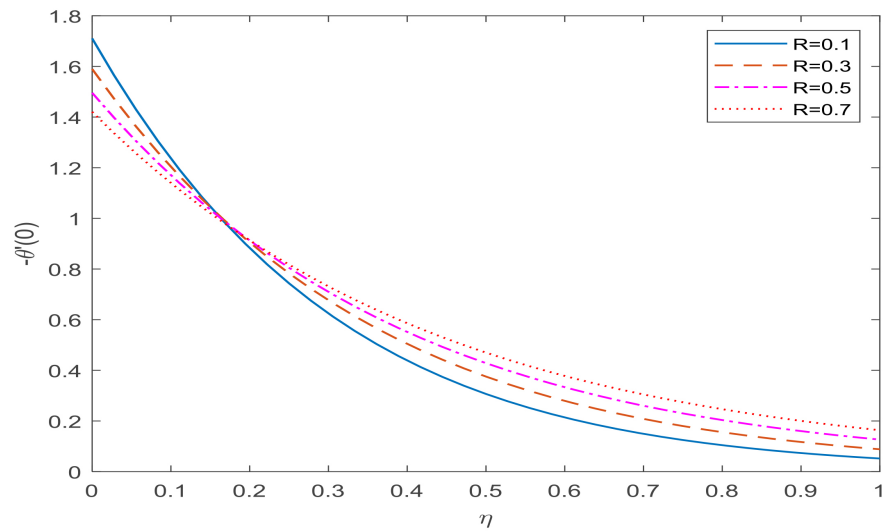


Figure 29. Influence of R on temperature gradient.

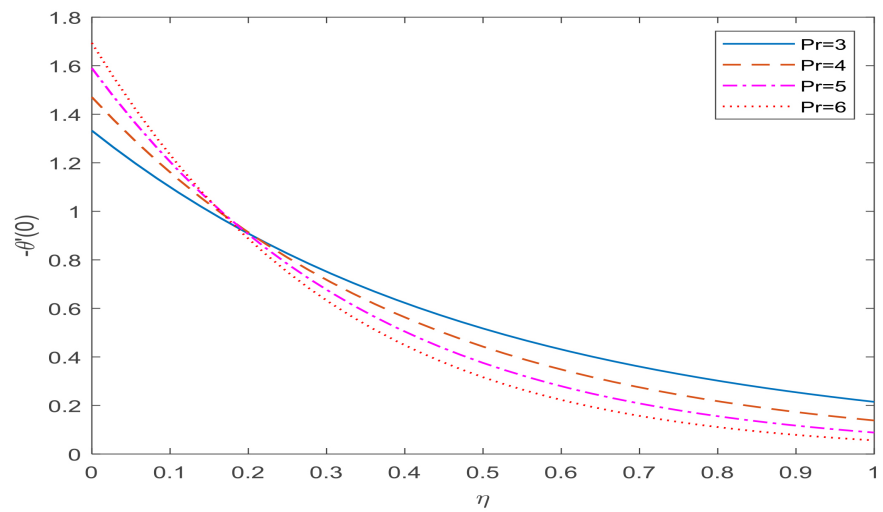


Figure 30. Influence of Pr on temperature gradient.

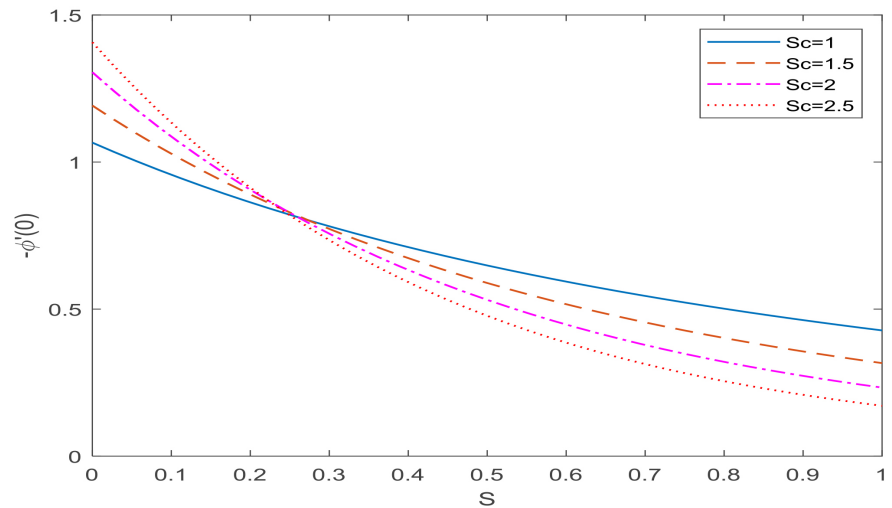


Figure 31. Influence of Sc on concentration gradient against suction parameter.

but increases after a certain distance η from the sheet in the presence of thermal Grashof number. The effect of radiation parameter on temperature gradient is portrayed in **Figure 29**, which shows that rate of heat transfer diminishes initially but enhances after a certain distance for η from the sheet. On the other hand, an opposite effect is observed for Prandtl number in **Figure 30**; that is temperature gradient accelerates initially but decelerates after a certain distance for η from the sheet. **Figure 31** highlights the effect of Schmidt number on concentration gradient against suction parameter. There exists intercept among the curves. It is found that Sherwood number increases initially but decreases for both large values of Schmidt number and suction parameter.

4. Conclusions

The problem of unsteady MHD mixed convective radiative flow over a porous sheet stretching exponentially with the effects of suction or blowing, multiple slips and internal heat generation or absorption is studied numerically. Some important results of the existing study are given below:

- The thermal Grashof number enhances the velocity and depreciates the temperature and concentration of the fluid. The mass Grashof number has the same effects as like thermal Grashof number on velocity, temperature and concentration profile respectively.
- The velocity temperature and concentration profile are increased with the rise in the unsteadiness parameter.
- The porosity and magnetic parameters have the same effects on fluid temperature and concentration profile as like velocity graph.
- The velocity slip parameter has the ability to reduce the fluid velocity and enhance the temperature and concentration of the fluid.
- As the thermal slip parameter increases the fluid temperature decreases.
- The concentration of the fluid is found to decline with the increasing values of the mass slip parameter.

- The thickness of the thermal boundary layer diminishes with growing Prandtl number and heat absorption parameter and while a reverse occurs with radiation parameter and heat generation parameter.
- Schmidt number diminishes the concentration of the fluid and elevates the Sherwood number.
- Suction parameter has an inclination to reduce the fluid velocity, temperature profile and concentration distribution; however blowing parameter acts reversely.

Conflicts of Interest

The authors declare no conflicts of interest regarding the publication of this paper.

References

- [1] Ahmad, K., Hanouf, Z. and Ishak, A. (2016) Mixed Convection Jeffrey Fluid Flow over an Exponentially Stretching Sheet with Magnetohydrodynamic Effect. *AIP Advances*, **6**, Article ID: 035024. <https://doi.org/10.1063/1.4945401>
- [2] Srinivasacharya, D. and RamReddy, C. (2011) Soret and Dufour Effects on Mixed Convection from an Exponentially Stretching Surface. *International Journal of Nonlinear Science*, **12**, 60-68.
- [3] Aman, F. and Ishak, A. (2012) Mixed Convection Boundary Layer Flow towards a Vertical Plate with a Convective Surface Boundary Condition. *Mathematical Problems in Engineering*, **2012**, Article ID: 453457. <https://doi.org/10.1155/2012/453457>
- [4] Isa, S.S.P.M., Arifin, N.M., Nazar, R., Bachok, N. and Ali, F.M. (2017) The Effect of Convective Boundary Condition on MHD Mixed Convection Boundary Layer Flow over an Exponentially Stretching Vertical Sheet. *Journal of Physics: Conference Series*, **949**, Article ID: 012016. <https://doi.org/10.1088/1742-6596/949/1/012016>
- [5] Patil, P.M., Latha, D.N., Roy, S. and Momoniat, E. (2017) Non-Similar Solutions of Mixed Convection Flow from an Exponentially Stretching Surface. *Ain Shams Engineering Journal*, **8**, 697-705. <https://doi.org/10.1016/j.asej.2015.10.012>
- [6] Ali, F.M., Khamat, A.N.A. and Junoh, M.M. (2021) Dual Solutions in Mixed Convection Stagnation-Point Flow over a Vertical Stretching Sheet with External Magnetic Field and Radiation Effect. *Journal of Advanced Research in Fluid Mechanics and Thermal Sciences*, **80**, 22-32. <https://doi.org/10.37934/arfmts.80.2.2232>
- [7] Dessie, H. and Kishan, N. (2014) MHD Effects on Heat Transfer over Stretching Sheet Embedded in Porous Medium with Variable Viscosity, Viscous Dissipation and Heat Source/Sink. *Ain Shams Engineering Journal*, **5**, 967-977. <https://doi.org/10.1016/j.asej.2014.03.008>
- [8] Ali, F., Sheikh, N.A., Saqib, M. and Khan, A. (2017) Hidden Phenomena of an MHD Unsteady Flow in Porous Medium with Heat Transfer. *Nonlinear Science Letters A*, **8**, 101-116.
- [9] Afify, A.A. and Elgazery, N.S. (2013) Effect of Double Dispersion on Non-Darcy Mixed Convective Flow over Vertical Surface Embedded in Porous Medium. *Applied Mathematics and Mechanics*, **34**, 1247-1262. <https://doi.org/10.1007/s10483-013-1742-6>
- [10] Tripathy, R.S., Dash, G.C., Mishra, S.R. and Hoque, M.M. (2016) Numerical Analysis of Hydromagnetic Micropolar Fluid along a Stretching Sheet Embedded in Porous Medium. *Journal of Applied Mathematics and Physics*, **7**, 1-10. <https://doi.org/10.1007/s10483-016-1742-6>

- ous Medium with Non-Uniform Heat Source and Chemical Reaction. *Engineering Science and Technology, an International Journal*, **19**, 1573-1581.
<https://doi.org/10.1016/j.jestch.2016.05.012>
- [11] Mahalakshmi, T., Nithyadevi, N. and Oztop, H.F. (2019) Numerical Study of Magnetohydrodynamic Mixed Convective Flow in a Lid-Driven Enclosure Filled with Nanofluid Saturated Porous Medium with Center Heater. *Thermal Science*, **23**, 1861-1873. <https://doi.org/10.2298/TSCI171105313N>
- [12] Krishna, M.V., Ahamad, N.A. and Chamkha, A.J. (2021) Hall and Ion Slip Impacts on Unsteady MHD Convective Rotating Flow of Heat Generating/Absorbing Second Grade Fluid. *Alexandria Engineering Journal*, **60**, 845-858.
<https://doi.org/10.1016/j.aej.2020.10.013>
- [13] Nazar, R., Ishak, A. and Pop, I. (2008) Unsteady Boundary Layer Flow over a Stretching Sheet in a Micropolar Fluid. *International Journal of Mathematical, Physical and Engineering Sciences*, **2**, 161-165.
- [14] Ibrahim, S.M. and Suneetha, K. (2016) Heat Source and Chemical Effects on MHD Convection Flow Embedded in a Porous Medium with Soret, Viscous and Joules Dissipation. *Ain Shams Engineering Journal*, **7**, 811-818.
<https://doi.org/10.1016/j.asej.2015.12.008>
- [15] Manjula, D. and Jayalakshmi, K. (2018) Slip Effects on Unsteady MHD and Heat Transfer Flow over a Stretching Sheet Embedded with Suction in a Porous Medium Filled with a Jeffrey Fluid. *International Journal of Research*, **7**, 609-623.
- [16] Mukhopadhyay, S., Bhattacharyya, K. and Layek, G.C. (2014) Mass Transfer over an Exponentially Stretching Porous Sheet Embedded in a Stratified Medium. *Chemical Engineering Communications*, **201**, 272-286.
<https://doi.org/10.1080/00986445.2013.768236>
- [17] Mukhopadhyay, S. (2011) Effects of Slip on Unsteady Mixed Convective Flow and Heat Transfer past a Porous Stretching Surface. *Nuclear Engineering and Design*, **241**, 2660-2665. <https://doi.org/10.1016/j.nucengdes.2011.05.007>
- [18] Sreelakshmi, K. and Nagendramma, V. (2015) Study of Thermophoresis on the MHD Flow Due to an Exponentially Stretching Sheet in the Presence of Viscous Dissipation. *Procedia Engineering*, **127**, 340-346.
<https://doi.org/10.1016/j.proeng.2015.11.379>
- [19] Mabood, F. and Shateyi, S. (2019) Multiple Slip Effects on MHD Unsteady Flow Heat and Mass Transfer Impinging on Permeable Stretching Sheet with Radiation. *Modelling and Simulation in Engineering*, **2019**, Article ID: 3052790.
<https://doi.org/10.1155/2019/3052790>
- [20] Islam, M.A., Ali, M.Y. and Gani, S.M.O. (2022) Unsteady Heat and Mass Transfer Slip Flow over an Exponentially Permeable Stretching Sheet. *Journal of Scientific Research*, **14**, 443-457. <https://doi.org/10.3329/jsr.v14i2.55577>
- [21] Brewster, M.Q. (1992) Thermal Radiative Transfer and Properties. John Wiley & Sons Inc., New York.